Published in final edited form as:
Cell Metab. 2010 January ; 11(1): 84–92. doi:10.1016/j.cmet.2009.11.003.

Irs1 Serine 307 Promotes Insulin Sensitivity in Mice

Kyle D. Copps[2], **Nancy J. Hancer**[2], **Lynn Opare-Ado**[2], **Wei Qiu**[2], **Cari Walsh**[2], and **Morris F. White**[1,2]

[1] Howard Hughes Medical Institute, Children's Hospital Boston, Harvard Medical School, Boston, MA 02115, USA

[2] Division of Endocrinology, Children's Hospital Boston, Harvard Medical School, Boston, MA 02115, USA

Summary

Phosphorylation of the insulin receptor substrates (Irs) on serine residues—typified by Ser307 of rodent Irs1—is thought to mediate insulin resistance. To determine whether Ser307 negatively regulates Irs1 *in vivo*, we generated knock-in mice in which Ser307 (human Ser312) was replaced with alanine (A/A). Unexpectedly, A/A mice that were fed a high fat diet developed more severe insulin resistance than control mice, accompanied by enhanced pancreatic compensation and impaired muscle insulin signaling. Chow-fed mice whose livers lacked Irs2, but retained a single knock-in allele (A/lox::LKO2) were profoundly insulin resistant (versus +/lox::LKO2 mice), and their hepatocytes showed impaired insulin signaling *ex vivo*. Similarly, mutant A307 Irs1 adenovirus only partially restored the response to injected insulin in mice lacking hepatic Irs1 and Irs2. Thus, contrary to the results of cell-based experiments, Ser307 in mice is a positive regulatory site that moderates the severity of insulin resistance by maintaining proximal insulin signaling.

Introduction

Insulin resistance, particularly in skeletal muscle, may underlie progression of Type 2 diabetes in otherwise healthy persons (Petersen et al., 2007). Tissue responsiveness to insulin requires the Irs1 and Irs2 proteins (Dong et al., 2008), which are phosphorylated by the insulin receptor (IR) on tyrosines to recruit the phosphatidylinositol 3’ kinase (PI3K). Production of PIP3 (phosphatidylinositol 3,4,5-trisphosphate) by PI3K in turn stimulates the activation of Akt by Pdk1, initiating diverse signaling pathways (White, 2006). By contrast, serine and threonine (Ser/Thr) phosphorylation of Irs1 by multiple kinases in response to inflammatory cytokines, fatty acids, and insulin itself can impair insulin signaling in cultured cells (Zick, 2005). Of more than 200 Ser/Thr residues in Irs1, around 30 are known to be phosphorylated in insulin-treated cells or human muscle (Giraud et al., 2007; Yi et al., 2007). Hyperactivation of the nutrient- and insulin-stimulated mTORC1→S6k1 pathway causes extensive Ser/Thr phosphorylation and degradation of Irs1 and diminished Akt activation (Harrington et al., 2004; Shah et al., 2004). However, reduced Irs1 protein

Corresponding author: Morris F. White Howard Hughes Medical Institute, Division of Endocrinology Children's Hospital Boston Harvard Medical School Karp Family Research Laboratories, Rm 4210 300 Longwood Avenue Boston, Massachusetts 02115, USA Phone: (617) 919-2846 Fax: (617) 730-0244 morris.white@childrens.harvard.edu.

expression is typically not seen in human diabetic muscles (reviewed in Leng et al., 2004). Consistent with the hypothesis that insulin resistance instead emerges from particular patterns of Irs-protein modification, phosphorylation of Ser312 and Ser636/639 of Irs1 is elevated in skeletal muscle of pre-diabetic humans (Morino et al., 2005), whereas the cognate sites (Ser307, 632/635) are hypo-phosphorylated in tissue from highly insulin-sensitive *S6k1*$^{-/-}$ mice.

In cultured cells, mutation of Ser307 was shown to protect against tumor necrosis factor alpha (TNFα)-induced inhibition of Irs1 tyrosine (Tyr) phosphorylation via the Jnk kinase pathway (Aguirre et al., 2000); thus, Ser307 phosphorylation is frequently cited as a cause of stress-induced insulin resistance. Increased Ser307 phosphorylation is seen in *ob/ob* and high-fat fed mice, which integrate the inflammatory, hyperinsulinemic, and dyslipidemic features of type 2 diabetes (Hirosumi et al., 2002; Um et al., 2004). Further, *ob/ob* mice lacking Jnk1 exhibit reduced Ser307 phosphorylation and improved insulin sensitivity, with decreased circulating insulin concentration (Hirosumi et al., 2002). In skeletal muscle of humans and rodents, infusion of triglyceride impairs insulin-stimulated glucose disposal through a mechanism involving decreased Irs1-associated PI3K activity (Kruszynska et al., 2002; Yu et al., 2002). In mice, this is accompanied by increased phosphorylation of Ser307 (Yu et al., 2002), potentially by the PKCθ kinase (Kim et al., 2004). Hyperinsulinemic-euglycemic clamp—which may mimic the hyperinsulinemia of diabetes—is also sufficient to stimulate phosphorylation of Ser307 and many other sites on Irs1 in human muscle (Yi et al., 2007).To experimentally address the function of Ser307 in whole animals, we prepared knock-in mice in which this residue could not be phosphorylated. Analysis of these mice indicates, surprisingly, that Irs1 Ser307 is required to maintain normal insulin signaling, particularly during nutrient and genetic stress.

Results

Generation of mutant and control knock-in mice

Mice lacking Ser307 in Irs1 (A/A mice) were generated by replacing the endogenous *Irs1* gene with a point-mutated copy (Ser307Ala, or A allele) (Figure S1A). Knock-in mice (S/S) bearing a non-mutated allele (S) were generated by the same method to control for the effect of a residual 66 bp fragment in the 3' non-coding region of the knock-in alleles (Figure S1B). Normal splicing of *Irs1* mRNA in knock-in mice was confirmed by RT-PCR, and genomic sequencing revealed no unexpected differences in *Irs1* non-coding or protein coding sequences (Figure S1C, A). Mouse embryo fibroblasts (MEFs) derived from e13.5 littermate A/A and S/S embryos were used to confirm mutation of Ser307 by immunoblot. Basal Tyr phosphorylation of Irs1 was high in both cell types, obscuring insulin-stimulated Tyr phosphorylation of Irs1; however, phosphorylation of Ser307 was evident at all times in S/S, but not A/A, MEFs (Figure 1A). Despite this difference, insulin-stimulated phosphorylation of Akt and its targets Foxo1 and Tsc2—as well as indirect target S6k—was indistinguishable between S/S and A/A MEFs (Figure 1B). Irs2 concentrations were also unaffected. Thus, the mutation of Ser307 did not markedly alter insulin signaling in these primary cells.

Analysis of glucose homeostasis in A/A mice

To evaluate the function of Ser307 in whole body glucose homeostasis, A/+ and S/+ mice were back-crossed to C57BL/6 mice, which are predisposed to diet-induced obesity and insulin resistance (Surwit et al., 1988). Male A/A, S/S and wild-type (WT, +/+) mice (n=11-17 per group) were fed a regular chow diet. The cumulative function of Irs1 in growth and development was examined at 4 months using dual X-ray absorptiometry (DEXA) (Figure 1C). Compared to +/+ mice, both S/S and A/A mice had slightly decreased

(~5-10%) body mass, length, and bone mineral density (BMD), but unchanged adiposity, revealing a small effect of knock-in at the *Irs1* locus independent of Ser307 status. Glucose and insulin tolerance tests (GTT, ITT), summarized areas under curves (AUC), were performed at 5 months of age. In GTTs, glucose excursion was slightly greater in A/A than in S/S or +/+ mice, reaching significance versus S/S mice (A/A, 2.47±.08 *vs.* S/S, 2.00±.12; p<.05) (Figure 1D). In ITTs—which measure the response to injected insulin—the AUC for A/A mice was insignificantly elevated, but the maximum drop in blood glucose in A/A mice (at 60 min.) tended to be less than in S/S mice (p=.10), and was significantly less than in +/+ mice (p<.05). By contrast, S/S and +/+ mice were indistinguishable by GTT or ITT.

Insulin resistance is compensated by increased insulin secretion and pancreatic β-cell hyperplasia to maintain normoglycemia. Although fasting blood glucose was equivalent in A/A, S/S, and +/+ mice (time=0 min., Figure 1D), the median fasting plasma insulin in A/A mice (465 pg/ml) was >2.5-fold higher than that in S/S mice (177 pg/ml, p=.07, *r*=–.44) or +/+ mice (163 pg/ml, p<.05, *r*=–.48) (Figure 1F). Despite marginal significance in the comparison of A/A and S/S insulin concentrations, the effect size (*r*) was consistent with a substantial effect of Ser307 status on their distributions. To limit the influence of extreme values, insulin concentrations were reanalyzed excluding tailing outliers (>1.5 times group interquartile ranges, Figure 1F). After trimming, the median insulin in A/A mice (404 pg/ml) was still significantly higher than in either control group (S/S mice: 175 pg/ml, p<.05, *r*=–.51; +/+ mice 159 pg/ml, p<.01, *r*=–.53). As in the GTT and ITT assays, no difference was seen between S/S and +/+ mice (NS, *r*=–.16), demonstrating that knock-in *per se* had no effect on insulin sensitivity. Compatible with these data, we previously observed normal fasting insulinemia in mice homozygous for the similarly-targeted $Irs1^{lox}$ (lox) conditional allele (Dong et al., 2008).

Ser307 protects mice against high-fat diet-induced insulin resistance

The strong positive skew of insulin concentrations in A/A mice implied that mutation of Ser307 allowed a transition to insulin resistance dependent upon other factors. To sensitively test for such an effect—while minimizing the influence of genetic variation—two cohorts of male A/A, A/+, and +/+ mice were either fed regular chow (chow, n=7-10/group) or switched to a high-fat diet (HFD, n=9-10/group) beginning at 4 weeks of age. Subsequent comparisons tested for effects of complete or partial absence of Ser307 in A/A or A/+ mice.

Consumption of HFD was equivalent between A/A, A/+, and +/+ mice (not shown), causing significant weight gain after ~8 weeks (Figure 2A). DEXA analysis of HFD-fed mice showed no effect of Ser307 mutation on body mass, length, or adiposity (p<.05, Figure S2A). Fasting blood glucose was increased on HFD for all groups, while fed glucose was nearly unaffected (Figure 2B). GTT and ITT assays at 20 weeks of age revealed no significant reduction in insulin sensitivity of chow-fed A/A or A/+ mice (Figure 2C, E). By contrast, HFD-fed A/A mice were significantly glucose intolerant (AUC: A/A mice, 4.79±.27; +/+ mice, 3.79±.20, p<.05, *r*=–.61), whereas glucose excursion of A/+ mice was between that of A/A and +/+ mice (Figure 2D). Responses of HFD-fed mice to insulin in the ITT followed the same pattern (Figure 2F); however, high within-group variance precluded a finding of significance [H(2) = 5.34, p=.07; *post hoc* comparisons omitted].

Robust evidence of insulin resistance in A/A and A/+ mice was seen in pancreatic adaptations to hyperglycemia (Figure 2G, H). In the small chow-fed cohort, both fasting insulin and β-cell area were absolutely, but insignificantly, higher in A/A and A/+ mice than in +/+ mice. However, on HFD the median fasting insulin concentrations of A/A and A/+ mice (1.28 and 1.67 ng/ml) were substantially elevated (~1.9-2.5-fold) over that of +/+ mice (0.68 ng/ml) (NS, *r*=–.47; and p<.025, *r*=–.66, respectively). Moreover, HFD caused pancreatic β-cell areas of both A/A and A/+ mice to increase significantly (~2.5-fold) over

that of +/+ controls ($p<.01$, $r=-.73$ and $p<.05$, $r=-.54$, respectively). In limited testing, we also found that homozygosity for the *Irs1* A allele had no effect on development of obesity and glucose intolerance in *ob/ob* mice (Figure S2D-E), in whose tissues Ser307 phosphorylation is elevated (Hirosumi et al., 2002). Thus substitution of Ser307 with alanine failed to ameliorate—and even exacerbated—insulin resistance caused by diet- and genetic-induced obesity.

Mutation of Ser307 fails to block HFD-induced desensitization of insulin signaling

Consistent with published data (Um et al., 2004), HFD increased both basal and insulin-stimulated Ser307 phosphorylation in muscle of +/+ and A/+ mice (Figure 3A). Insulin-stimulated Akt T308 phosphorylation—dependent on both Irs1 and Irs2—was not significantly diminished in HFD-fed A/A muscles (Figure 3B). To further gauge the effects of reduced Ser307 phosphorylation, Irs1 Tyr phosphorylation (pTyr) and PI3 kinase (p85) binding were compared in Irs1 immunoprecipitates (IPs). In chow-fed mouse muscles, pTyr and p85 binding were roughly equivalent between +/+, A/+ and A/A samples. By contrast, HFD-fed mouse muscles of each genotype showed decreased insulin stimulation (fold over basal) of Irs1 Tyr phosphorylation and p85 binding, and this desensitization of insulin signaling was more pronounced in muscle from A/+ and A/A mice than from +/+ mice (Figure 3C). Anti-Irs2 IPs showed equivalent signaling via this pathway in chow-fed mouse muscles, with similar degrees of desensitization by HFD across all genotypes (Figure 3D). In the liver, the effects of Ser307 mutation on signaling did not follow as clear a pattern. Insulin-stimulated binding of p85 to Irs1 and Irs2 was moderately reduced in chow-fed A/A liver (Figure S2B, C), but this did not translate into decreased Akt (Thr308) phosphorylation. However, Akt phosphorylation was reduced significantly in HFD-fed A/A liver (Figure S2B). Thus, although signaling experiments revealed only modest differences between A/A and control tissues, the overall pattern of proximal insulin signaling was incompatible with an insulin-sensitizing effect of reduced Ser307 phosphorylation.

The insulin- and nutrient-stimulated kinase S6k1 phosphorylates Irs1 at Ser302, as well as other putatively inhibitory sites (Harrington et al., 2004).Thus, its activating phosphorylation was assayed in liver of chow-fed mice that were fasted overnight and re-fed for 1-2 hours. However, S6k Thr389 phosphorylation did not differ between A/A and +/+ mice (Figure 3E) and immunoblotting also failed to show elevated Irs1 Ser302 phosphorylation in A/A liver (not shown). Further, no significant difference was observed in the phosphorylation of nine Irs1 Ser/Thr sites (save Ser307) between Irs1-deficient primary hepatocytes reconstituted with WT or mutant (A307) Irs1 adenovirus (Figure 3F). Thus, insulin resistance in A/A mice appeared to owe specifically to mutation of Ser307, rather than to activation of feedback pathways that influence phosphorylation at other tested sites.

Reduced activity of $A307^{Irs1}$ is revealed by deletion of hepatic Irs2

We previously reported that mice with *Alb-Cre*-mediated deletion of *Irs2* in hepatocytes (LKO2 mice) are nearly normal, whereas mice lacking hepatic *Irs1* and *Irs2* (LDKO) are profoundly insulin resistant (Dong et al., 2008). Because insulin resistance in chow-fed A/A mice could be obscured by normal Irs2 signaling, we re-examined the insulin sensitivity of +/+ and A/A mice on the LKO2 mouse background. By crossing A/+ mice to LDKO mice, we produced (Cre^+) male LKO2 mice whose livers retained a WT or mutant *Irs1* allele in double or single copy. These mice were compared at 24 weeks of age, with LDKO littermates included for qualitative comparison. In GTTs, glucose tolerance was correlated with *Irs1* allelic dose and identity: +/+::LKO2 > +/lox::LKO2 > A/A::LKO2 > A/lox::LKO2 > LDKO (Figure 4A, C). Strikingly, A/lox::LKO2 mice—but not +/lox::LKO2—showed severe glucose intolerance similar to that of LDKO mice, suggesting that $A307^{Irs1}$ only weakly mediated the insulin signal. Further, A/A::LKO2 mice were significantly glucose

intolerant versus +/+::LKO2, and were indistinguishable from +/lox::LKO2 mice. In ITTs (Figure 4B, C), A/lox::LKO2 mice—but not +/lox::LKO2—showed significant insulin resistance that was only slightly improved compared to DKO mice; as in the GTT assay, A/A::LKO2 mice responded similarly to +/lox::LKO2 mice. Fasting insulin concentrations—indicative of compensation for insulin resistance—were in the same order as glucose excursion in the GTT (Figure 4D). Fasting insulinemia was significantly increased ($p<.05$) in both A/lox::LKO2 and A/A::LKO2 mice. As in the GTT and ITT assays, A/A::LKO2 mice did not differ significantly from +/lox::LKO2 mice.

Defective insulin signaling by A307^{Irs1} in hepatocytes *ex vivo*

The profound insulin resistance of A/lox::LKO2 mice was of particular interest because, excluding their hepatocytes, these mice were the practical equivalent of A/+ mice, in which we observed glucose tolerance, insulin sensitivity, and fasting insulin similar to those in WT mice (*i.e.*, A/+ vs. +/+, chow diet, Figure 2C, E, G). Thus, it appeared that the insulin resistance of A/lox::LKO2 versus +/lox::LKO2 mice owed specifically to reduced function of the A307^{Irs1} protein in liver hepatocytes. To test this hypothesis, primary hepatocytes were isolated from 10 week-old A/lox::LKO2 and +/lox::LKO2 males, at which time these mice did not yet differ by GTT (data not shown). These cells expressed equivalent levels of Irs1, and stimulation with insulin resulted in similar degrees of Tyr phosphorylation in Irs1 IPs (Figure 4E, F). In contrast, insulin-stimulated binding of the p85 (regulatory) and p110α (catalytic) subunits of PI3K to Irs1 was significantly reduced in A/lox::LKO2 hepatocytes ($p<0.05$). As in muscles of HFD-fed A/A mice, however, downstream activation of Akt (T308 phosphorylation) was not significantly impaired.

A307^{Irs1} adenovirus incompletely restores insulin sensitivity in LDKO mice

To control for peripheral or developmental influences on liver A307^{Irs1} function, we reconstituted livers of LDKO mice using WT or mutant Irs1 adenoviruses (Ad-WT and Ad-A307; n=11, 12). Rescue of insulin sensitivity in the infected mice was gauged by GTT and ITT; for qualitative comparison, we included non-infected control mice (FF; identical to LDKO, but lacking *Alb-Cre*). Perhaps owing to incomplete pancreatic compensation in the young (6 to 8-week-old) LDKO recipients, neither virus restored normal glucose tolerance in GTTs (not shown). By contrast, insulin sensitivity in ITTs was better restored in mice that received WT Irs1 adenovirus (Figure 4G), and the maximum hypoglycemic response was significantly greater in Ad-WT- than in Ad-307-infected mice (30 min. time point, Figure 4H). These data are compatible with reduced function of the A307^{Irs1} protein, and further support that Ser307 or its phosphorylation contributes to normal signaling by Irs1.

Discussion

The requirement of Ser307 for insulin sensitivity in knock-in mice runs counter to prevailing notions about the function of this phosphorylation site. To date, however, almost all of the evidence linking Ser307 phosphorylation to insulin resistance in whole animals has been formally correlative in nature. In one exceptional study, it was recently shown that transgenic mice expressing triply-mutated (Ser 302/307/612→Ala) Irs1 in their skeletal muscle are protected against development of high-fat diet-induced insulin resistance (Morino et al., 2008); however, the incompletely reductive design of this study makes it impossible to infer the specific contribution of Ser307. In contrast, we observed significant insulin resistance in high-fat-fed Ser307Ala knock-in mice (A/A), suggesting that the enhanced sensitivity of Ser 302/307/612 →Ala transgenic mice may owe to mutation of Ser302, Ser612, or both sites together.

In established cells that overexpress the IR and Irs1, Ser307 was previously shown to be required for the modest inhibition of Irs1 Tyr phosphorylation caused by TNFα treatment (Aguirre et al., 2000). However, another cell-based study found no effect of a phospho-mimetic Ser307Asp mutation on insulin-stimulated glucose disposal, suggesting that Ser307 phosphorylation does not contribute substantially to insulin resistance (Weigert et al., 2008). Compatible with this result, we observed mild effects of the Ser307Ala mutation in chow-fed A/A and A/+ mice that nevertheless progressed to insulin resistance upon high fat feeding or deletion of hepatic Irs2. In further contrast with established cell lines (Aguirre et al., 2000; Weigert et al., 2008), both HFD-fed A/A mouse muscles and primary hepatocytes from A/lox::LKO2 mice displayed slightly reduced or unchanged tyrosyl phosphorylation of $A307^{Irs1}$ following insulin stimulation. In both cases, this was accompanied by decreased insulin-stimulated binding of PI3K to Irs1, without a marked decrease in Akt phosphorylation. In muscles of HFD-fed A/A mice, this may have owed to Akt activation via the Irs2 pathway; however, it is also possible that we did not choose the appropriate time to monitor Akt phosphorylation, which is typically rapidly saturated and long-lasting. We conclude that Ser307 in whole animals promotes insulin sensitivity through a moderate, but physiologically significant, effect to maintain PI3 kinase binding to Irs1.

As in other animal-based studies (e.g.,Um et al., 2004), we noted significant stimulation of Ser307 phosphorylation by insulin, even in tissues of HFD-fed mice. Further, in primary hepatocytes infected with WT Irs1 adenovirus, Ser307 was strongly phosphorylated by insulin treatment. While these data are compatible with a positive role of Ser307 in signaling by Irs1, in other experiments we found that only a fraction of the total Irs1 in muscles of chow-fed mice or WT hepatocytes is phosphorylated on Ser307 by insulin stimulation (K.C., M.W.). Thus, Ser307 phosphorylation is not a *sine qua non* for signaling via Irs1, but may function to maintain signaling by the Ser307-phosphorylated fraction. Fluctuation in the size of this fraction—for example, as influenced by diet—might therefore have modulated the severity of physiologic and signaling defects observed in our studies. The phosphorylation of other Ser/Thr sites is also likely to have affected Irs1 function; however, we did not observe markedly different phosphorylation of WT and A307 Irs1 at eight other Ser/Thr sites in adenovirus-infected hepatocytes, suggesting that the insulin resistance of A/A mice owed primarily to the effect of Ser307 status. Thus, despite clear upregulation of Ser307 phosphorylation in animal models of insulin resistance, this modification may have an adaptive, rather than pathogenic function. Extension of the knock-in mouse approach used here to other Ser/Thr sites will help to determine how common, or rare, this function might be.

Experimental Procedures

Mice and diets

Mouse procedures were approved by the Children's Hospital IACUC. The conditional Irs^{lox} allele was previously described (Dong et al., 2008). Production and genotyping of $Irs^{A/A}$ (A/A) and $Irs^{S/S}$ (S/S) knock-in mice are detailed in the Supplement. The diets (PMI Nutrition Intl., Richmond, IN) were: Chow (Prolab Isopro, #5P76; 14 kcal% of energy from fat of diverse sources) and HFD (Surwit 5800-B, #58R3; 58 kcal% in fat from hydrogenated coconut oil). Mice in Figures 1-3 were progeny of inbred (C57BL/6; n=9+) $Irs1^{A/+}$ or $Irs1^{S/+}$ pairs. Breeding of the mice in Figure 4 is detailed in the Supplement.

Metabolic assays

For GTT, mice were fasted for 16 h, blood was drawn, and mice were injected intra-peritoneally (IP) with 2g/kg glucose. For ITT, blood was drawn beginning ~3h after the end of dark phase, after which mice were fasted 4 h, then injected IP with insulin (Lilly,

Humulin R). Areas under curves (AUC) were calculated by summation of trapezoids. Plasma insulin was measured by ELISA (Crystal Chem.) using rat insulin standard.

Isolation of primary cells

MEF cells were isolated as described (Bruning et al., 1997) using embryos from *Irs1*$^{A/S}$ (A/S) mating pairs. Frozen primary MEFs (p0) were thawed and grown to 70% confluency, then reseeded in DMEM plus 10% FBS on plates corresponding to treatments shown. Upon confluency, MEFs were washed twice with serum-free DMEM and incubated a further 16 h without serum before insulin treatment. Isolation and culture of mouse hepatocytes is detailed in the Supplement.

Tissue collection and analysis

Pancreatic β-cell area was measured as described (Kushner et al., 2004) in 5 to 6 month-old male chow- and HFD-fed mice (n=6 and 7-10/group). For immunoblots, mice were fasted 16 h, then injected via the vena cava with 5 U of Humulin R (Lilly) under anesthesia; tissues were collected after 5 min. and frozen in liquid nitrogen. To assay S6K phosphorylation, fasted mice were instead re-fed for 1 or 2 h and sacrificed by CO_2 asphyxiation; consumption of chow was confirmed by monitoring blood glucose and stomach contents. Tissues were lysed and analyzed as described (Dong et al., 2008) using antibodies described in the Supplement..

Adenovirus injection

Male LDKO mice (6-8 week-old) were injected via the tail vein with 2×10^{10} pfu of soft agar-titred Ad-WT or Ad-A307. The ITT assay was performed 5 d after virus injection using 0.8 U/kg of insulin.

Statistical treatment and graphs

Significance was assessed at the 95% level using the Kruskal-Wallis (K-W) and Mann-Whitney (M-W) tests (SPSS, v16). For three or more groups, an overall difference in data location of at least one of the groups was assayed using the K-W (H) test; where found, this was followed by pairwise M-W (U) tests (with Bonferroni correction of α) to identify differences between groups. For two groups, the M-W test was used. Except in Figure 4, where reduction of allelic number or the mutant allele was expected to worsen insulin sensitivity, p values were calculated from the two-tailed X^2 distribution. Effect size (Pearson's *r*) was calculated from the *z* score of the M-W test. In Figures 3A-D and S2B-C, estimated means normalized to the average concentration of the protein of interest (Irs1, Irs2, or tubulin for Akt) were determined with a generalized linear model (SPSS v16) assuming a normal distribution of the response, an identity link, and the concentration of the protein of interest as a covariate. In each case, the Bonferroni p-values are reported to correct for multiple comparisons. Except as indicated, bars and error bars in graphs represent the mean and standard error of the mean.

Supplementary Material

Refer to Web version on PubMed Central for supplementary material.

Acknowledgments

This work was supported by NIH grant DK43808 and the Howard Hughes Medical Institute. We thank Matthew Dow for technical assistance in production of knock-in mice.

References

Aguirre V, Uchida T, Yenush L, Davis R, White MF. The c-Jun NH(2)-terminal kinase promotes insulin resistance during association with insulin receptor substrate-1 and phosphorylation of Ser(307). J. Biol. Chem. 2000; 275:9047–9054. [PubMed: 10722755]

Bruning JC, Winnay J, Cheatham B, Kahn CR. Differential signaling by insulin receptor substrate 1 (IRS-1) and IRS-2 in IRS-1-deficient cells. Mol. Cell Biol. 1997; 17:1513–1521. [PubMed: 9032279]

Dong XC, Copps KD, Guo S, Li Y, Kollipara R, DePinho RA, White MF. Inactivation of hepatic Foxo1 by insulin signaling is required for adaptive nutrient homeostasis and endocrine growth regulation. Cell Metab. 2008; 8:65–76. [PubMed: 18590693]

Giraud J, Haas M, Feener EP, Copps KD, Dong X, Dunn SL, White MF. Phosphorylation of Irs1 at SER-522 inhibits insulin signaling. Mol. Endocrinol. 2007; 21:2294–2302. [PubMed: 17579213]

Harrington LS, Findlay GM, Gray A, Tolkacheva T, Wigfield S, Rebholz H, Barnett J, Leslie NR, Cheng S, Shepherd PR, Gout I, Downes CP, Lamb RF. The TSC1-2 tumor suppressor controls insulin-PI3K signaling via regulation of IRS proteins. J Cell Biol. 2004; 166:213–223. [PubMed: 15249583]

Hirosumi J, Tuncman G, Chang L, Gorgun CZ, Uysal KT, Maeda K, Karin M, Hotamisligil GS. A central role for JNK in obesity and insulin resistance. Nature. 2002; 420:333–336. [PubMed: 12447443]

Kim JK, Fillmore JJ, Sunshine MJ, Albrecht B, Higashimori T, Kim DW, Liu ZX, Soos TJ, Cline GW, O'Brien WR, Littman DR, Shulman GI. PKC-theta knockout mice are protected from fat-induced insulin resistance. J Clin Invest. 2004; 114:823–827. [PubMed: 15372106]

Kruszynska YT, Worrall DS, Ofrecio J, Frias JP, Macaraeg G, Olefsky JM. Fatty acid-induced insulin resistance: decreased muscle PI3K activation but unchanged Akt phosphorylation. J. Clin. Endocrinol. Metab. 2002; 87:226–234. [PubMed: 11788651]

Kushner JA, Haj FG, Klaman LD, Dow MA, Kahn BB, Neel BG, White MF. Islet-sparing effects of protein tyrosine phosphatase-1b deficiency delays onset of diabetes in IRS2 knockout mice. Diabetes. 2004; 53:61–66. [PubMed: 14693698]

Leng Y, Karlsson HK, Zierath JR. Insulin signaling defects in type 2 diabetes. Rev. Endocr. Metab Disord. 2004; 5:111–117. [PubMed: 15041786]

Morino K, Neschen S, Bilz S, Sono S, Tsirigotis D, Reznick RM, Moore I, Nagai Y, Samuel V, Sebastian D, White MF, Philbrick W, Shulman GI. Muscle-specific IRS-1 Ser->Ala transgenic mice are protected from fat-induced insulin resistance in skeletal muscle. Diabetes. 2008; 57:2644–2651. [PubMed: 18633112]

Morino K, Petersen KF, Dufour S, Befroy D, Frattini J, Shatzkes N, Neschen S, White MF, Bilz S, Sono S, Pypaert M, Shulman GI. Reduced mitochondrial density and increased IRS-1 serine phosphorylation in muscle of insulin-resistant offspring of type 2 diabetic parents. J. Clin. Invest. 2005; 115:3587–3593. [PubMed: 16284649]

Petersen KF, Dufour S, Savage DB, Bilz S, Solomon G, Yonemitsu S, Cline GW, Befroy D, Zemany L, Kahn BB, Papademetris X, Rothman DL, Shulman GI. The role of skeletal muscle insulin resistance in the pathogenesis of the metabolic syndrome. Proc. Natl. Acad. Sci. U. S. A. 2007; 104:12587–12594. [PubMed: 17640906]

Shah OJ, Wang Z, Hunter T. Inappropriate Activation of the TSC/Rheb/mTOR/S6K Cassette Induces IRS1/2 Depletion, Insulin Resistance, and Cell Survival Deficiencies. Curr Biol. 2004; 14:1650–1656. [PubMed: 15380067]

Surwit RS, Kuhn CM, Cochrane C, McCubbin JA, Feinglos MN. Diet-induced type II diabetes in C57BL/6J mice. Diabetes. 1988; 37:1163–1167. [PubMed: 3044882]

Um SH, Frigerio F, Watanabe M, Picard F, Joaquin M, Sticker M, Fumagalli S, Allegrini PR, Kozma SC, Auwerx J, Thomas G. Absence of S6K1 protects against age- and diet-induced obesity while enhancing insulin sensitivity. Nature. 2004; 431:200–205. [PubMed: 15306821]

Weigert C, Kron M, Kalbacher H, Pohl AK, Runge H, Haring HU, Schleicher E, Lehmann R. Interplay and effects of temporal changes in the phosphorylation state of serine-302, -307, and

-318 of insulin receptor substrate-1 on insulin action in skeletal muscle cells. Mol. Endocrinol. 2008; 22:2729–2740. [PubMed: 18927238]

White, MF. The Molecular Basis of insulin action.. In: DeGroot, LJ.; Jameson, JL., editors. Endocrinology. Elsevier; Philadelphia: 2006. p. 975-1000.

Yi Z, Langlais P, De Filippis EA, Luo M, Flynn CR, Schroeder S, Weintraub ST, Mapes R, Mandarino LJ. Global assessment of regulation of phosphorylation of insulin receptor substrate-1 by insulin in vivo in human muscle. Diabetes. 2007; 56:1508–1516. [PubMed: 17360977]

Yu C, Chen Y, Cline GW, Zhang D, Zong H, Wang Y, Bergeron R, Kim JK, Cushman SW, Cooney GJ, Atcheson B, White MF, Kraegen EW, Shulman GI. Mechanism by which fatty acids inhibit insulin activation of insulin receptor substrate-1 (IRS-1)-associated phosphatidylinositol 3-kinase activity in muscle. J. Biol. Chem. 2002; 277:50230–50236. [PubMed: 12006582]

Zick Y. Ser/Thr phosphorylation of IRS proteins: a molecular basis for insulin resistance. Sci. STKE. 2005; 2005:e4.

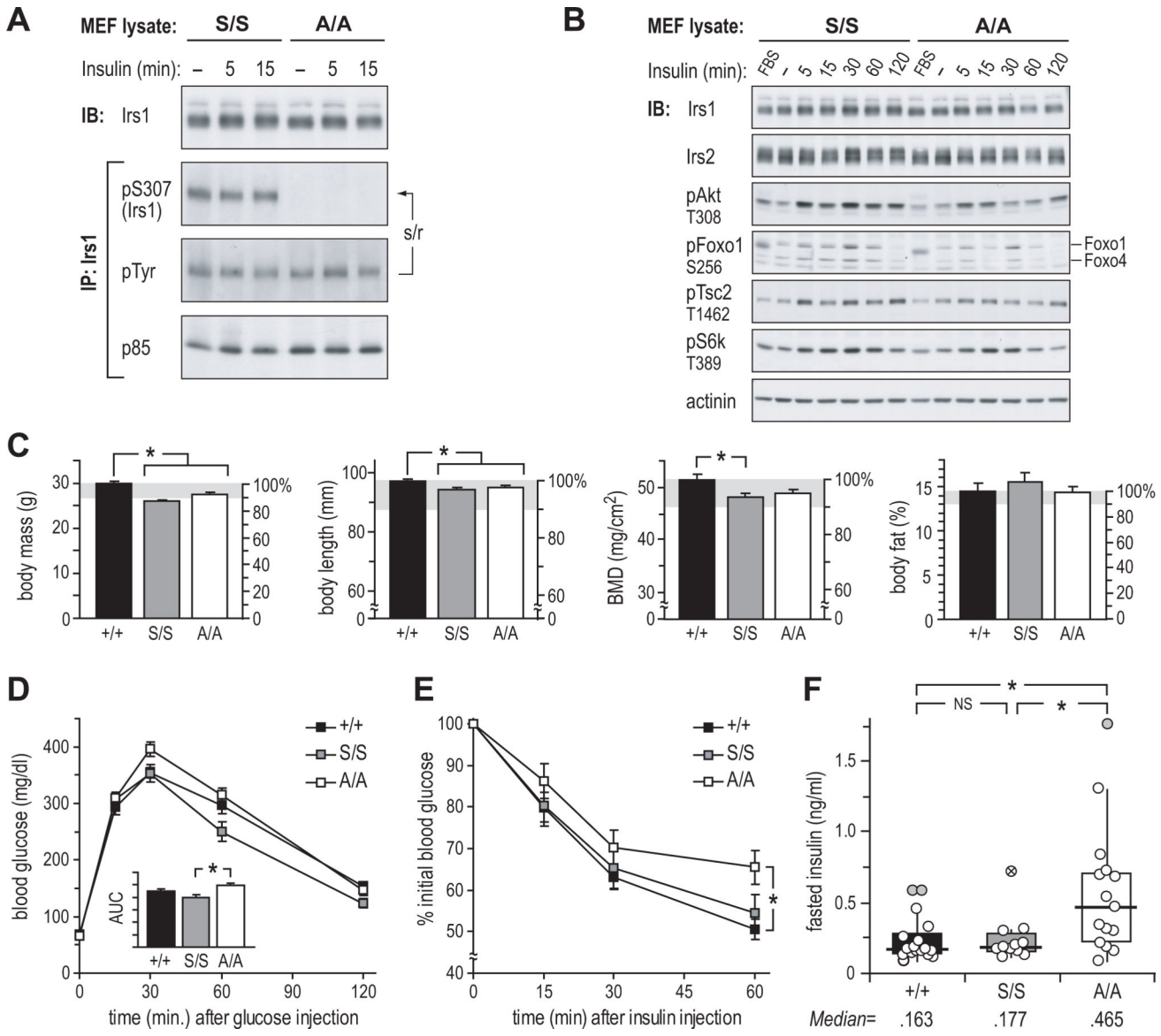

Figure 1. Irs1 Ser307Ala Knock-in Mice Are Insulin Resistant Versus Control Knock-in and WT Mice

(A and B) Immunoblot analysis of insulin signaling in control (S/S) and mutant (A/A) knock-in mouse embryonic fibroblasts (MEF); cells were maintained in 10% serum (FBS), or fasted (–) 16h before treatment with 100nM insulin; IP: immunoprecipitation; IB: immunoblot; s/r: stripped/reprobed membrane.

(C) DEXA analysis of 16-week-old WT (+/+), control knock-in (S/S), and mutant knock-in mice (A/A). Bars show mean ± SEM; BMD: bone mineral density.

(D and E) Glucose tolerance test and (E) insulin tolerance test in 5-month-old chow-fed mice; AUC: area under curve (mean ± SEM, arbitrary units).

(F) Fasted plasma insulin at time=0 of GTT; box: interquartile range (IQR); horizontal bar: median; vertical bar: 95% of distribution. The exclusion of tailing outliers (> 1.5×IQR: ● and > 3×IQR: ⊗) gave trimmed medians of 159 (+/+), 175 (S/S) and 404 pg/ml (A/A), yielding significance ($p < 0.05$) for the comparison of A/A *vs.* S/S insulin distributions.

* = $p < 0.05$.

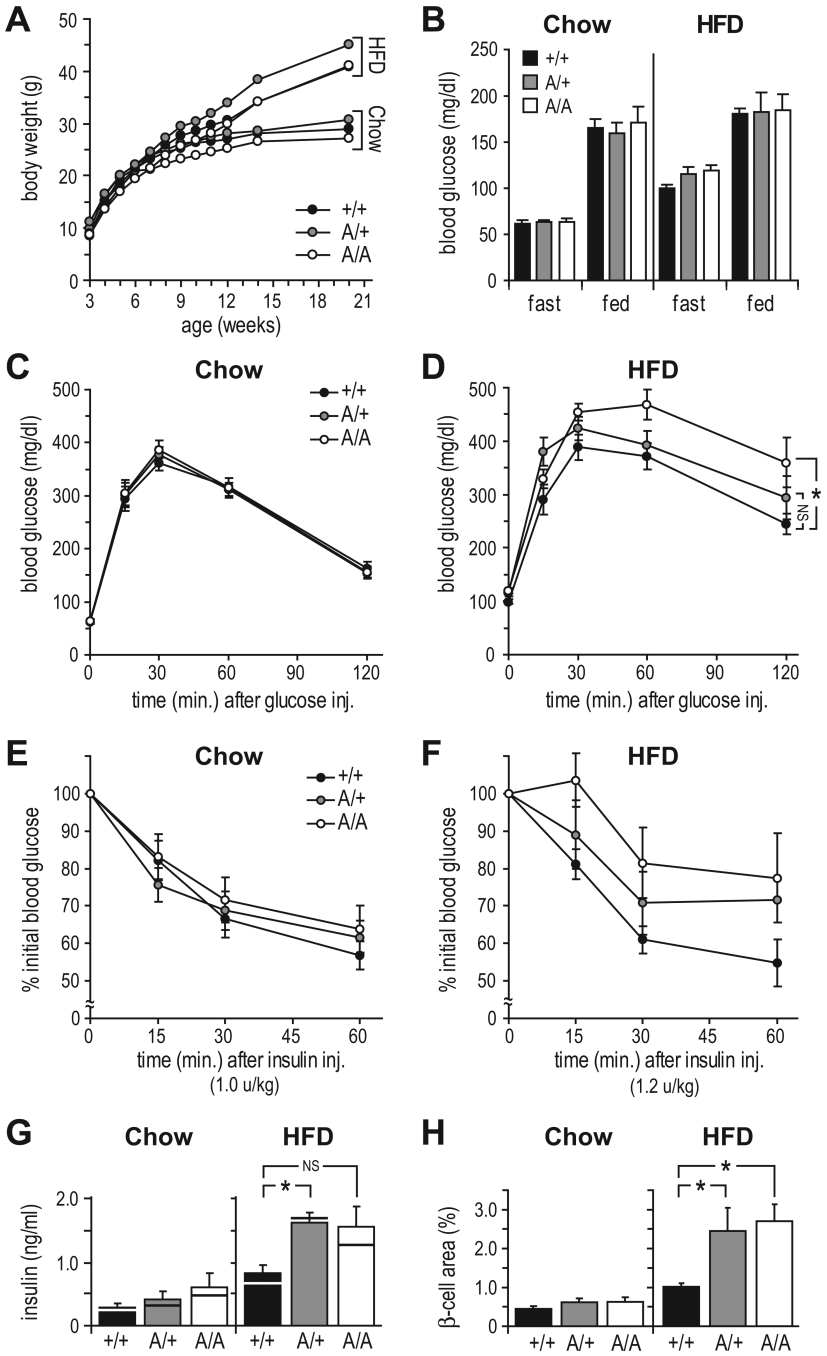

Figure 2. Ser307 Protects Mice Against High Fat Diet-Induced Insulin Resistance

(A) Body weight gain (mean ± SEM) in mice fed regular chow (Chow) or high fat diet (HFD).

(B) Effect of diet on fasting and fed blood glucose (mean ± SEM) at 5 months of age.

(C-F) Glucose tolerance tests (C-D) and insulin tolerance tests (E-F) on 5-month-old mice maintained on chow or HFD. Graphs show mean ± SEM at each point; * = $p < 0.05$, NS=not significant for area under curve.

(G) Fasting plasma insulin concentrations (mean ± SEM) at time=0 of GTT in chow- and HFD-fed mice; horizontal bars: median values.

(H) β-cell area (pixel %, mean ± SEM) in pancreatic sections from chow- and HFD-fed mice.
* = $p < 0.05$, NS=not significant.

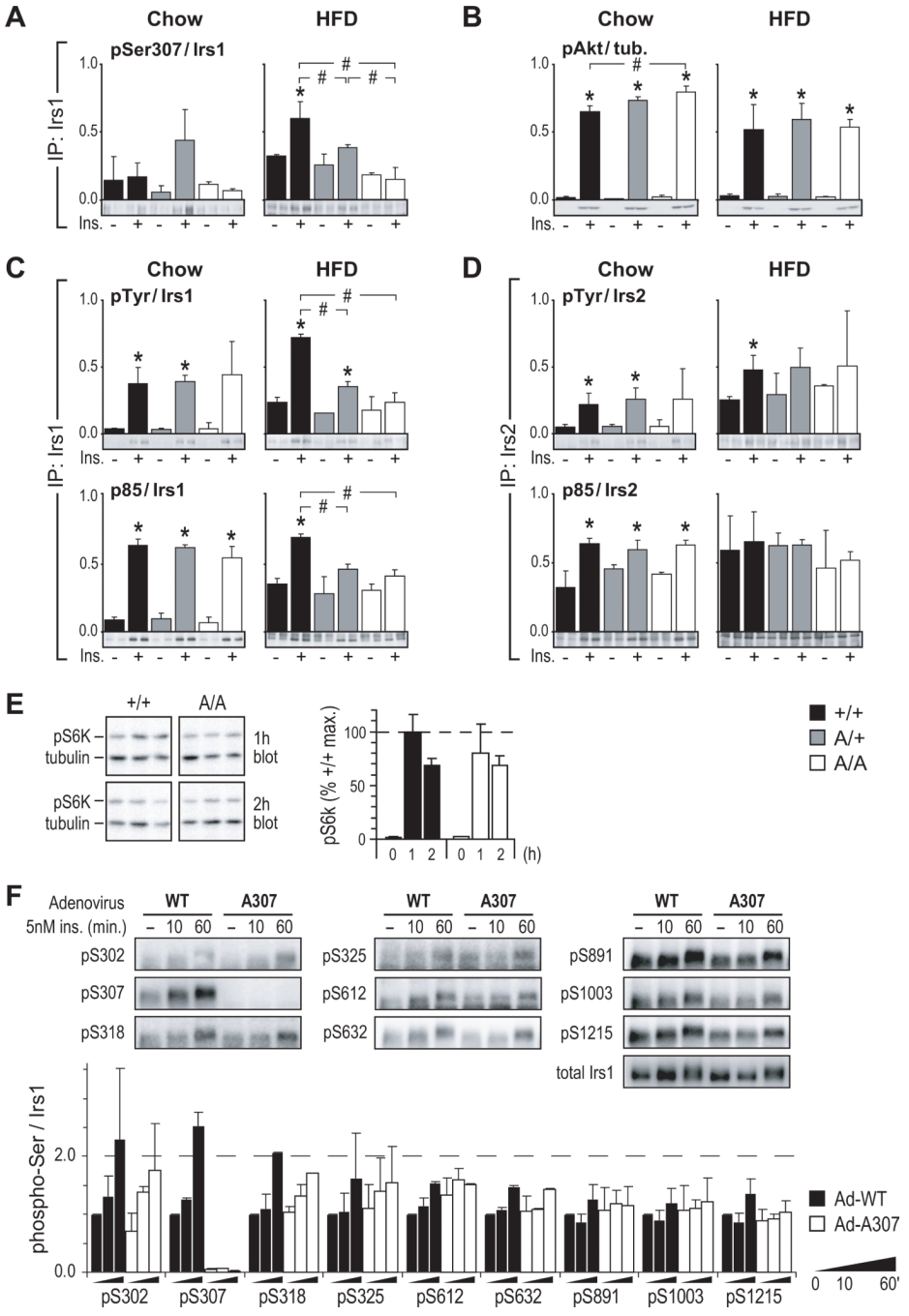

Figure 3. Mutation of Ser307 Fails To Protect Against HFD-Induced Desensitization of Insulin Signaling

(A) Immunoblot analysis of basal (–) and insulin-stimulated (+) Ser307 phosphorylation in hindlimb muscle of 5 to 6-month-old mice fed chow (Chow) or high-fat diet (HFD). Immunoprecipitated Irs1 (IP: Irs1) was detected using a phospho-specific antibody against 15 residues of mouse Irs1.

(B) Corresponding Akt (Thr308) phosphorylation.

(C-D) Immunoprecipitation (IP:) and immunoblot analysis of insulin signaling by Irs1 (C) or Irs2 (D) in muscle of chow- and HFD-fed mice; pTyr: phosphotyrosine.

In panels A-D, the estimated means of phosphotyrosine, p85, or phospho-Thr308^{Akt} signals (see methods) were normalized to the average total Irs1, Irs2, or tubulin concentrations; * = significant difference (Bonferroni $p<0.05$) vs. unstimulated; # = significant difference (Bonferroni $p<0.05$) between indicated insulin-stimulated samples.
(E) Immunoblot analysis of p70 S6 kinase (Thr389) phosphorylation (mean ± SEM) in livers of overnight fasted mice re-fed for 1 or 2 h. Mice were previously fed chow diet.
(F) Immunoblot analysis of Irs1 Ser/Thr phosphorylation. Primary hepatocytes from mice lacking hepatic Irs1 and Irs2 ('LDKO' Dong et al., 2008) were infected with wild-type (Ad-WT) or mutant (Ad-A307) Irs1 adenovirus for 24 h, then treated as shown after 16 h of serum starvation. Relative Irs1 phosphorylation (mean ± SEM) at each site is graphed as fold of Ad-WT-infected cells without insulin (–).

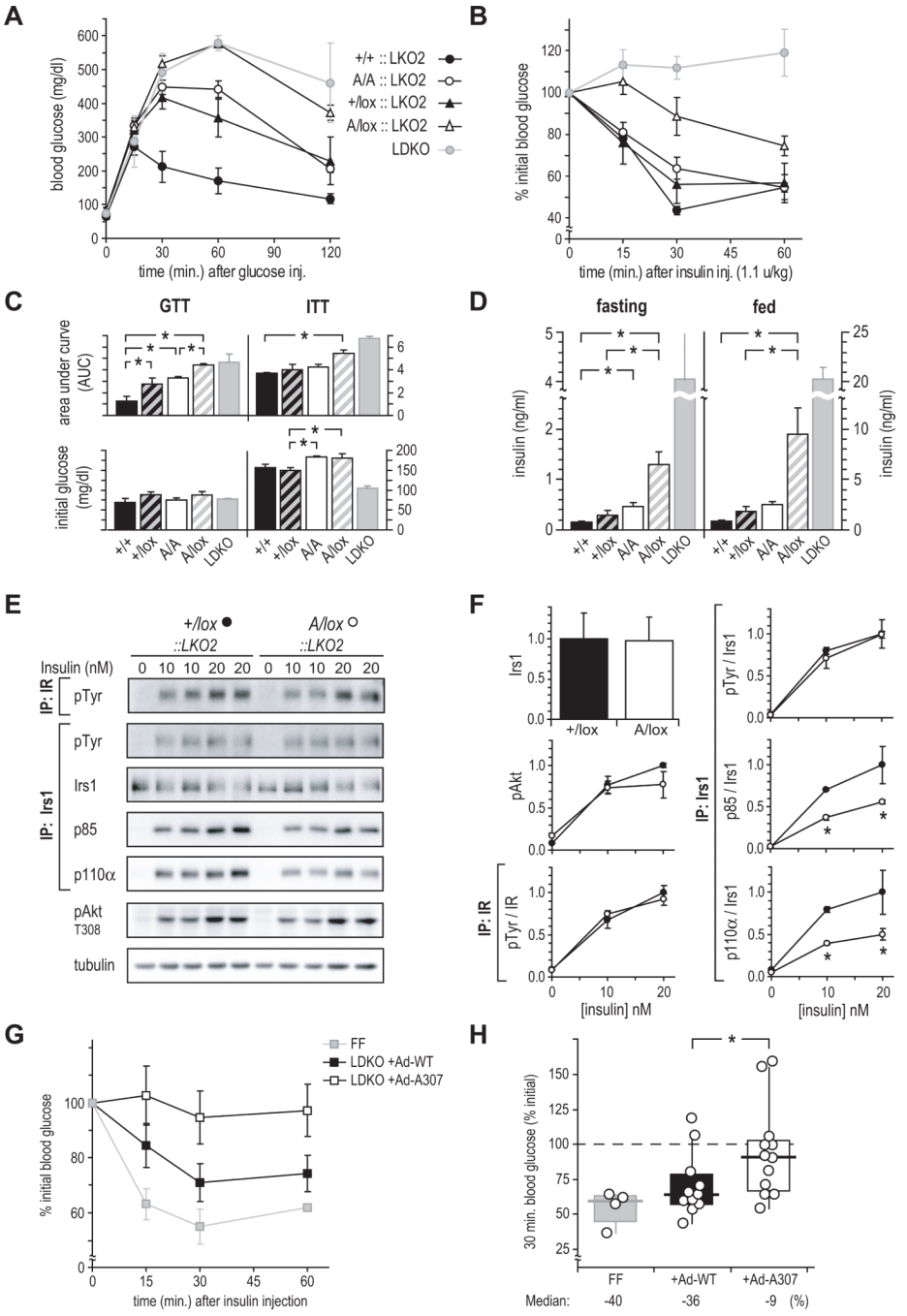

Figure 4. *In vivo* and *ex vivo* function of A307^{Irs1} in the absence of Irs2-mediated signaling

(A and B) GTT and (B) ITT of 6-month-old mice lacking hepatic Irs2 (LKO2::) with varying *Irs1* allelic composition. Owing to the action of Cre recombinase on the *Irs1^{lox}* allele (lox), A/lox::LKO2 and +/lox::LKO2 mice retained a single active *Irs1* allele.

(C and D) Areas under GTT and ITT curves (AUC), with corresponding initial blood glucose and (D) insulin concentrations. LDKO mice are shown for qualitative comparison. Labels show *Irs1* genotype only. Data are mean ± SEM; * = $p < 0.05$.

(E) Insulin signaling in hepatocytes of 10-week-old +/lox::LKO2 and A/lox::LKO2 mice. IP: immunoprecipitation; IB: immunoblot.

(F) Quantitation of blots in E; &25cf;: +/lox::LKO2; ○: +/lox::LKO2. Signals were normalized to the average value in 20 nM insulin-stimulated +/lox::LKO2 cells measured in duplicate in two separate experiments. Data represent mean values ± standard deviation. * = $p < 0.05$ by (Student t test).
(G) Insulin tolerance (mean ± SEM at each point) in LDKO mice infected with wild-type (+Ad-WT) or mutant (+Ad-A307) Irs1 adenovirus. Insulin tolerance in non-infected, Cre-negative double-floxed mice (FF) is shown for qualitative comparison.
(H) Maximum hypoglycemic response (time=30 min) during the insulin tolerance test in G; box: interquartile range; horizontal bar: median; vertical bar: 95% of distribution. * = $p < 0.05$.